PCCP

Accepted Manuscript

ROYAL SOCIETY OF CHEMISTRY

www.rsc.org/pccp

Coordination properties of metal chelator clioquinol to Zn^{2+} studied by static DFT and ab initio molecular dynamics

Luis Rodríguez-Santiago,[a,*] Jorge Alí-Torres,[b] Pietro Vidossich,[a,c,*] Mariona Sodupe[a]

[a]*Departament de Química, Universitat Autònoma de Barcelona, Bellaterra 08193, Spain*

[b]*Departamento de Química, Universidad Nacional de Colombia - Sede Bogotá, 111321, Colombia*

[c]*Computational Biophysics, German Research School for Simulation Sciences (joint venture of RWTH Aachen University and Forschungszentrum Jülich, Germany), D-52425 Jülich, Germany*

Corresponding authors: Luis.Rodriguez.Santiago@uab.cat, vido@klingon.uab.es

Abstract

Several evidences supporting the role of metal ions in amyloid aggregation, one of the hallmarks of Alzheimer's disease (AD), have turned metal ion chelation into a promising therapeutic treatment. The design of efficient chelating ligands requires proper knowledge of the electronic and molecular structure of the complexes formed, including their hydration properties. Among various potential chelators, clioquinol (5-chloro-7-iodo-8-hydroxyquinoline, CQH), has been evaluated with relative success in *in vitro* experiments and even in phase 2 clinical trials. Clioquinol interacts with Zn(II) to lead to a binary metal/ligand 1:2 stoichiometric complex in which the phenolic group of CQH is deprotonated, resulting in $Zn(CQ)_2$ neutral complexes, to which additional water molecules may coordinate. In the present work, the coordinative properties of clioquinol in aqueous solution have been analyzed by means of static, minimal cluster based DFT calculations and explicit solvent *ab initio* molecular dynamics simulations. Results from static calculations accounting for solvent effects by means of polarized continuum models suggest that the preferred metal coordination environment is tetrahedral $Zn(CQ)_2$, whereas *ab initio* molecular dynamics simulations point to quasi degenerate penta $Zn(CQ)_2(H_2O)$ and hexa $Zn(CQ)_2(H_2O)_2$ coordinated complexes. The possible reasons for these discrepant results are discussed.

Introduction

One of the neuropathological hallmarks of Alzheimer disease (AD) is the presence of extra-cellular neurotoxic deposits (senile plaques) formed by the aggregation of the Aβ peptide, a 39- to 43-residue degradation fragment of the much larger precursor protein (APP).[1] Although the origin of these deposits is still not clear, and multiple factors such as pH, metal ions and oxidative stress have been reported to trigger their formation, several evidences highlight the importance of metal cations. *Post-mortem* studies of AD patients show high concentration (~mM) of metal cations such as Fe^{3+}, Cu^{2+} and Zn^{2+}.[2] Moreover, *in vitro* experiments have shown that Zn^{2+} and Cu^{2+} promote Aβ aggregation[3,4] and that the aggregates can be solubilized by using metal chelators,[5] thereby suggesting that the metal cation is critical for stabilizing the aggregates. These evidences have rendered metal-ion chelation therapy a promising therapeutic treatment.[6,7] Among the various potential ligands reported to date, clioquinol (5-chloro-7-iodo-8-hydroxyquinoline, CQH, see Scheme 1), has been evaluated with relative success in *in vitro* experiments with brain tissues, in transgenic mice[8] and even in a completed small-scale phase 2 clinical trial.[9]

The development of the new generation of metal chelators has recently focused on the design of multifunctional ligands; i.e., ligands that are not only capable of efficiently coordinate the metal cations (as CQH does) but also have functional groups that help reaching the target improving their performance.[10] Towards this end, knowledge of the physico-chemical properties of a lead compound such as CQH is essential to develop new drug molecules with improved activity. In the case of metal chelators, the determination of stability constants requires knowledge of the coordination environment of the metal cation and of its hydration properties. To date, the coordination chemistry of CQH toward transition metal cations in aqueous solution has been little investigated. It is known that the coordination of CQH to both Zn^{2+} and Cu^{2+} ions involves deprotonation of the phenolic group, which results in neutral ML_2 species. Furthermore, the X-ray crystal structure of the Zn^{2+} complex[11] shows that the metal cation is penta-coordinated by the oxygen and nitrogen atoms of the two anionic ligands and by a water molecule, in an approximately trigonal bipyramidal environment. However, this coordination environment may change in aqueous solution. Indeed, zinc is known to have a very flexible coordination behavior, forming complexes with coordination numbers of 4, 5 and 6.[12] X-ray absorption spectroscopies (EXAFS or

XANES) are capable of provide valuable information on metal coordination environment in solution. Unfortunately, no such data is available for Zn/cliquinol complexes.

The main goal of the present work is to study the coordination properties of Zn^{2+} interacting with CQH in aqueous solution by means of first principles molecular modeling techniques. Specifically, static DFT calculations, based on reduced model systems and accounting for solvent effects within a continuum approach, and *ab initio* molecular dynamics simulations using explicit solvent molecules have been carried out. Moreover, and for comparison, the intrinsic coordination properties in gas phase have also been analyzed. Results show that the preferences for a given coordination highly depends on the computational strategy used to model the system. Namely, gas phase results show that the penta-coordinated $[Zn(CQ)_2(H_2O)]$ complex is the preferred one, whereas implicit solvent calculations seem to indicate that tetrahedral $[Zn(CQ)_2]$ is the most favorable structure. In contrast, *ab initio* molecular dynamics simulations considering explicit solvent molecules show that the complex prefers penta or hexa-coordination, more in line with the observed X-ray structure.

Methods

Static calculations. Full geometry optimizations and harmonic frequency calculations of the different systems in gas phase were carried out by means of density functional theory (DFT) using the B3LYP[13–15] and BLYP[15,16] functionals. DFT methods have been widely used for the study of transition-metal containing systems and, in particular, the hybrid B3LYP functional has been shown to be a cost-effective method for studying this kind of systems.[17] The pure GGA BLYP functional was also considered and compared to B3LYP since molecular dynamic simulations were carried out at this level of theory. Gas phase results show that both methods provide similar results, differences on relative energies being always smaller than 2 kcal mol^{-1}. Thus, and for consistency with the molecular dynamics simulations, results discussed along the manuscript will always refer to the BLYP functional. Results obtained with B3LYP are given in the Supplementary Information. Solution phase geometry optimizations and harmonic frequency calculations were carried out using the same BLYP and B3LYP density functional methods combined with two different continuum models to account for solvent effects. In particular, we used the CPCM model[18–20] combined with a cavity

generated using the united atom topological model on radii optimized at the HF/6-31G(d) level of theory,[21] and the SMD method of Marenich et al.[22] in which the "D" stands for "density" to denote that the full solute electron density is used without defining partial atomic charges. Although larger differences, up to 5 kcal mol^{-1}, on the relative stabilities of the different complexes are observed with the two continuum models, the observed trends are the same and thus, only the results obtained with SMD will be discussed in the main manuscript. Results obtained with CPCM are given in the Supplementary Information. The nature of the stationary points was characterized by vibrational analysis.

The standard 6-31++G(d,p) basis set has been employed for H, C, N, O and Cl atoms. For I, the LANL2DZ core pseudo-potentials and the associated basis sets was used.[23] For Zn we considered the (15s11p6d1f)/[10s7p4d1f] basis, based on the (14s9p5d) primitive set of Wachters,[24] supplemented with one s, two p and one d diffuse and one f polarization function.[24–26] Thermodynamic corrections were obtained assuming an ideal gas behaviour, unscaled harmonic vibrational frequencies, and the rigid rotor approximation by standard statistical methods. Gibbs free energies in solution were computed using as the reference state 1 mol L^{-1} at a temperature of 298.15 K. All calculations were performed through the Gaussian 09 package.[27]

Dynamic calculations. Ab initio molecular dynamics simulations (AIMD) were performed according to the Born-Oppenheimer approach using the CP2K program.[28] Simulations were carried out at the BLYP-D3 level, i.e. by using the BLYP[15,16] functional supplemented with the Grimme's[29] D3 correction for dispersion. This functional has been widely used for simulations on liquid water (see e.g. references [30] and [31]) and is the functional that better performs when the dispersion correction is included.[29]

The BLYP gas phase optimized structures of the $[Zn(CQ)_2]$ and $[Zn(CQ)_2H_2O]$ complexes were used as starting points for the simulations. Complexes were solvated with 254 and 253 water molecules, respectively, in a cubic box of size L = 19.960 Å, which reproduces the density of water at ambient conditions, and treated under periodic boundary conditions. Subsequently, a 250 ps classical MD simulation, keeping fixed the coordinates of the complex, was undertaken to equilibrate water molecules around the metal complex. The force field was based on the flexible simple point-charge water model of Wu et al. [32], and on non bonded OPLS parameters.[33] Point charges for the

organometallic frame were obtained through RESP calculations[34] at the gas-phase BLYP minima. The final conformation was used as starting point for the AIMD simulation. For each system, a 23 ps AIMD simulation was performed at constant volume and constant temperature. A time step of 0.5 fs for the integration of the equations of motion and a Nose-Hoover thermostat[35,36] with coupling constant 16.68 fs were used. The reference temperature was set to 350 K in order to guarantee the liquid state of the solvent.[37,38] The Quickstep algorithm[39] was used to solve the electronic structure problem using a double-zeta plus polarization (DZVP) basis set[40] to represent the orbitals and plane waves (up to 300 Ry) for the electron density. Core electrons were described by pseudopotentials[41,42] and wave function optimization was achieved through the orbital transformation method (the convergence criterion for the electronic gradient was set to $5 \cdot 10^{-7}$).[43]

Free energy calculations. Umbrella sampling simulations were performed to reconstruct the free energy profile (FEP) associated to water coordination to $[Zn(CQ)_2]$. The collective variable used is the coordination number between zinc and all water oxygen atoms ($CN_{Zn\text{-}Ow}$), and is defined as:[44]

$$CN_{Zn-Ow} = \sum_{1}^{N_O} \frac{1 - \left(\frac{d_{Zn-O}}{d_0}\right)^8}{1 - \left(\frac{d_{Zn-O}}{d_0}\right)^{16}}$$

where $d_{Zn\text{-}O}$ is the Zn-O distance; d_0 = 2.6 Å and N_O = 254. $CN_{Zn\text{-}Ow}$ varies between ≈ 0 for $Zn(CQ)_2$ to ≈ 2 for $Zn(CQ)_2(H_2O)_2$. The sampling along the coordinate was split into 14 overlapping windows by applying a harmonic restraint centered at distinct values of the reaction coordinate and with force constant 480 kcal mol^{-1}. For each window 10 ps simulation were accumulated. The free energy profile was reconstructed using the Umbrella Integration method.[45] System configurations to initialize each window were extracted from a metadynamics[46,47] simulation, performed using the same collective variable on which a history dependent repulsive potential was acting to promote sampling of configurational space.

Results

Gas phase calculations

We have pursued two strategies with respect to the model systems used for the calculation of relative stabilities of hexa-, penta- and tetra-coordinated complexes. In one, we have considered the sequential dissociation of water molecules from the hexa-coordinated $[Zn(CQ)_2(H_2O)_2]$ complex, keeping the dissociated water molecule within the cluster. In the other, we have considered $[Zn(CQ)_2(H_2O)]$ and $[Zn(CQ)_2]$, without water molecules in the second shell. The most stable optimized gas phase BLYP structures for the different coordination geometries are shown in Figure 1 along with their relative Gibbs energies (ΔG^0_{gas}). The full set of optimized structures at the BLYP and B3LYP levels of theory is given in the Supplementary Information (Figures S1 and S2) along with the reaction energies corresponding to the interconversion between the different structures (Figure S3).

The $[Zn(CQ)_2]\cdot 2H_2O$ complex shows tetrahedral coordination at the metal center with both clioquinol ligands in an almost perpendicular arrangement. Second shell water molecules interact with the CQ^- ligands through hydrogen bonds with the clioquinol oxygen atoms and more weakly with the –CH groups, the $O\cdots H_2O$ and -$CH\cdots OH_2$ distances being 1.913 and 2.334 Å, respectively. In $[Zn(CQ)_2(H_2O)]\cdot H_2O$ the coordination environment of zinc is approximately trigonal bipyramid with the phenolic oxygens occupying the axial positions and the two nitrogens and the water oxygen in the equatorial plane. In this configuration, which is found to be the most stable one, the second shell water molecule is interacting with the metal coordinating water and the oxygen atom of one of the ligands. Another less stable configuration with the water molecule interacting with the oxygen atom of one of the CQ^- moieties and one -CH group of the second CQ^- was also localized 5 kcal mol^{-1} higher in energy (Figure S2). Finally, the $[Zn(CQ)_2(H_2O)_2]$ complex exhibits a distorted octahedral geometry with the water molecules in trans position and the CQ^- molecules in the equatorial plane. All attempts to optimize an alternative structure with the coordinating water molecules in cis arrangement collapsed to $[Zn(CQ)_2(H_2O)]\cdot H_2O$ with one water molecule directly coordinated to the metal center and the other one in the second coordination sphere. Noteworthy, minor changes are observed in the Zn coordination when complexes are optimized removing second shell waters from the models.

Relative free energies given in Figure 1 for $[Zn(CQ)_2(H_2O)_{2-n}]\cdot H_2O_n$ species show that the penta-coordinated $[Zn(CQ)_2(H_2O)]\cdot H_2O$ complex is the most stable structure. The hexa-coordinated complex lies 9.6 kcal mol^{-1} higher in energy whereas the tetracoordinated one $[Zn(CQ)_2]\cdot 2H_2O$ is found to be 5.5 kcal mol^{-1} less stable. However, when water dissociation is considered, i.e., the processes $[Zn(CQ)_2(H_2O)_n] \rightarrow [Zn(CQ)_2(H_2O)_{n-1}] + H_2O$, n = 2 and 1, the tetra-coordinated complex is the preferred one, since both reactions, from the hexa- to the penta- and from the penta- to the tetra-coordinated complex are exergonic (for $[Zn(CQ)_2(H_2O)_2] \rightarrow [Zn(CQ)_2(H_2O)] + H_2O$ the reaction energy is −7.7 kcal mol^{-1}, and for $[Zn(CQ)_2(H_2O)] \rightarrow [Zn(CQ)_2] + H_2O$ it is −2.7 kcal mol^{-1}). Note that the difference between the complete dissociation of the first water molecule to yield $[Zn(CQ)_2(H_2O)]$ (−7.7 kcal mol^{-1}) and the transfer of the water molecule from the first to the second coordination shell ($[Zn(CQ)_2(H_2O)]\cdot H_2O$) (-9.6 kcal mol^{-1}) is only 1.9 kcal mol^{-1}, due to enthalpy-entropy compensation effects. On the contrary, the reaction energy is 5.5 kcal mol^{-1} for $[Zn(CQ)_2(H_2O)]\cdot H_2O \rightarrow [Zn(CQ)_2]\cdot 2H_2O$ and −2.7 kcal mol^{-1} for $[Zn(CQ)_2(H_2O)] \rightarrow [Zn(CQ)_2] + H_2O$, resulting in different minimum free energy structures depending on whether the coordinating water molecules are considered fully dissociated or not.

Implicit solvent calculations

The same model systems as for the gas phase calculations were used for implicit solvent calculations. The optimized structures of the complexes with different metal coordination, with and without additional water molecules in the second shell, are shown in Figure 2. It can be observed that these structures exhibit the same metal coordination environment as those found in the gas phase calculations. Nevertheless, for certain complexes solvent effects cause the appearance of additional conformers close in energy to the most stable ones. These structures are shown in Figures S4 to S9 of the Supplementary Information.

The $[Zn(CQ)_2]\cdot 2H_2O$ and $[Zn(CQ)_2]$ complexes show tetrahedral coordination at the metal center as for systems in gas phase. Noticeably, however, for $[Zn(CQ)_2]$ an additional minimum with a square planar coordination was found 4 kcal mol^{-1} above the tetrahedral geometry (see Figure S4). For the penta-coordinated $[Zn(CQ)_2(H_2O)]\cdot nH_2O$ species (n=0 and 1), in addition to the trigonal bipyramid structure with the oxygens in

the axial positions observed in gas phase, other structures were found when including solvent effects. In particular, for $[Zn(CQ)_2(H_2O)]\cdot H_2O$, three different structures were located, one with a square based pyramid structure, with the second shell water molecule interacting with the complex through the phenolic oxygen, and two trigonal bipyramid structures which show similar geometrical features than the gas phase corresponding structures. For $[Zn(CQ)_2(H_2O)]$ additional trigonal bipyramid minima were located with one oxygen and one nitrogen or two nitrogens in the axial positions (see Figure S6). All these structures, however, lie very close in energy, the largest difference being 0.9 kcal mol^{-1}. Finally for the hexacoordinated metal complex, we located an octahedral minimum with the water molecules in trans similar to that found in gas phase.

Relative free energies (ΔG^*_{sol}) shown in Figure 2 indicate that the tetracoordinated complex is the preferred metal coordination, both when considering second shell waters in the model or not. Reaction energies associated to moving the metal coordinated water molecules to the second shell $[Zn(CQ)_2(H_2O)_2] \rightarrow [Zn(CQ)_2(H_2O)_{2-n}]\cdot nH_2O$ (n=1 and 2) are exergonic. This is in contrast to that found in gas phase, for which the pentacoordinated $[Zn(CQ)_2(H_2O)]\cdot H_2O$ structure was found to be the most stable and is due to the changes induced on metal-water, ligand-water and water-water interactions upon considering the polarized continuum model. Indeed, comparison between optimized $[Zn(CQ)_2(H_2O)_{2-n}]\cdot nH_2O$ (n=1 and 2) structures in gas phase and in solution indicates that inclusion of solvent effects with the polarized continuum model SMD increases the Zn-O distance, whereas it decreases ligand-water hydrogen bond distances.

Explicit solvent simulations.

Two simulations were carried out starting from the gas phase BLYP optimized structures of $[Zn(CQ)_2(H_2O)]$ (simulation A) and $[Zn(CQ)_2]$ (simulation B).

$[Zn(CQ)_2(H_2O)]$ (simulation A) remains penta-coordinated throughout the simulation. The structure of the complex oscillates between square based pyramid and trigonal bipyramid with either the oxygens or the nitrogens in the axial positions. These structures were found to be almost degenerate in implicit solvent calculations (see Supplementary Information). The radial distribution function of water O atoms (O_w)

with respect to Zn g(Zn-O_w), shown in Figure 3a, presents a narrow peak at 2.10 Å, which integrates to 1.0, in agreement with the maintenance of the coordination by one water molecule.

In simulation B the initially tetra-coordinated complex evolves to increased coordination of the metal center. As shown in Figure 4, after 3 ps of simulation a water molecule, initially at about 4 Å from the metal, binds to the Zn atom and remains at a coordinating distance during the rest of the simulation. A second water molecule, initially at about 5 Å, also coordinates to the metal after 13 ps of simulation, resulting in a distorted octahedral geometry with the water molecules in cis position as shown in Figure 5. Accordingly, the g(Zn-O_w) graph shows a wider peak centered at 2.21 Å, which integrates to 1.3 oxygen atoms.

Of interest is also the interaction of solvent molecules with the CQ^- ligands, in particular with their phenol O atoms. The RDF of H atoms of water (H_w) with respect to the O atoms of the Zn-clioquinol (Figure 3b) shows a well-defined peak at 1.83 Å in simulation A and 1.81 Å in simulation B, indicating the formation of hydrogen bonds between the complex and the solvent molecules. The peak of simulation A integrates to 1.7, that is, each oxygen atom of the complex is solvated by almost 2 solvent molecules. In simulation B the peak integrates to a slightly lower value, 1.4, because for certain arrangements of the CQ ligands solvent molecules are excluded from the region around O ligand atoms (fluctuations bring the C-H group of the pyridine ring of one CQ ligand closer to the O of the other CQ ligand).

The free energy profile for water coordination to Zn was computed by means of an umbrella sampling simulation (see Methods section for details) and is shown in Figure 6. Interestingly, and in agreement with the result from the plain *ab initio* simulations, no minimum is found for values of $CN_{Zn\text{-}Ow}$ around 0, that is, the tetra-coordinated structure does not correspond to a minimum of this free energy surface. This finding disagrees with the outcome of gas phase and implicit solvent calculations where tetra-coordinated structures were located and found to be the most stable in most setups. The minimum of the profile corresponds to a flat, wide area with values of $CN_{Zn\text{-}Ow}$ from 1.2 to 1.8; that is, penta- and hexa-coordinated complexes seem to be degenerate. Again, this is in contrast to what is observed in the previous static calculations. Gas phase and implicit solvent calculations predicted the hexa-coordinated

structure to be less stable than the penta-coordinated one by 3.5-12.7 kcal mol^{-1} depending on the method and model used.

Discussion

Coordination of clioquinol to zinc leads to $Zn(CQ)_2$ neutral complexes. Given the variability observed in Zn coordination, further coordination by solvent molecules may take place in aqueous solution. Knowledge of the coordination environment of $Zn(CQ)_2$ adducts in solution is of central relevance for modeling studies addressing the chelating properties of CQ or the interactions between Zn, CQ and peptides. In this context, the X-ray crystallographic structure of the Zn complex shows an additional water ligand coordinated to the metal cation, thus giving rise to a $[Zn(CQ)_2H_2O]$ complex.[11] However, the extent to which crystallographic studies are representative of solution conditions is questionable. Here, we have used state of the art molecular modeling techniques to get a deeper insight into the coordinative state of $Zn(CQ)_2$ in aqueous solution. Calculations were based on Density Functional Theory (DFT) and considered models of increasing complexity. Quite disappointingly, it turned out that the size of the model considered has a considerable impact on the energetics of the $[Zn(CQ)_2(H_2O)_n]$ complexes, and no consistent picture emerged on which should be considered the most stable one.

For minimal models, the potential energy of binding does not compensate the reduction in translational entropy upon fragment binding (about 10 kcal mol^{-1} for a water molecule at 300 K), resulting in free energy estimates that favor lower coordination numbers (Figure 1b). Including bulk solvent effects as a continuum does not change this picture (Figure 2b).

In order to reduce the entropic penalty for binding, the dissociating fragment may be kept in the model. In the present case, this means that water molecule(s) relocate in the second coordination shell. The Zn-O_w bond is converted in ligand – H_wO_w hydrogen bond(s) and the preference of the water molecule for a first or second coordination environment depends on the relative strength of these interactions. In the present case, this approach also leads to low coordination numbers (four, see Figure 2)

When enough explicit solvent molecules are included in the model to mimic bulk conditions, the H-bonding properties of ligand atoms are saturated, and thus these

are no more competing interactions for a water molecule, which may conveniently prefer to coordinate Zn or reside in the bulk solution. From this perspective, the use of explicit solvent models would appear more appropriate to investigate metal – solvent interactions.[48] Unfortunately, this comes with an increased computational cost. Because of the large number of atoms in the model, a sampling method such as molecular dynamics is required, and special techniques have to be used for free energy estimates. An intermediate situation would be to use an extended cluster model that includes enough water molecules to saturate the H-bonds of the first shell ligand atoms. This approach has been pursued for instance in a study of Cu hydroxide hydration, in which the geometry at Cu in $[Cu(OH)(H_2O)_n]^+$ clusters turned to be square-planar four-coordinated for $n < 8$,[49] whereas for n=18, i.e. in the presence of two hydration shells, the five-coordinate square-pyramidal geometry was determined to be the most favorable one. While computation of properties e.g. spectroscopic parameters, usually benefit form extended clusters[50] it should be noted that this approach does not eliminate surface effects, which may be particularly severe when the interest is focused on the energetics of processes taking place at the metal center.

Conclusions

Clioquinol is a metal chelating ligand that has proven efficient to inhibit the aggregation of beta-amyloid induced by Zn(II) ions. Experimental studies show that CQH interacts with Zn(II) to lead to a binary metal/ligand 1:2 stoichiometric complex in which the phenolic group of CQH is deprotonated, resulting in $Zn(CQ)_2$ neutral complexes. X-yay diffraction studies on the crystal structure of Zn complexes formed with CQH indicate that the metal cation is coordinated by the oxygen and nitrogen atoms of the two anionic ligands and by a water molecule, in an approximately trigonal bipyramidal environment. However, considering the flexible coordination behavior of Zn, which is known to form complexes with coordination numbers of 4, 5 and 6, this coordination environment may change in aqueous solution. In the present work, the coordinative properties of clioquinol in aqueous solution have been analyzed by means of static DFT calculations and ab initio molecular dynamics simulations. Results from static calculations including solvent effects with the SMD polarized continuum model suggest that the preferred metal coordination environment is tetrahedral, whereas the more realistic ab initio molecular dynamics simulations suggest that the penta $Zn(CQ)_2(H_2O)$ and hexa

$Zn(CQ)_2(H_2O)_2$ coordinated complexes are major quasi degenerate structures and thus they are expected to coexist in aqueous solution. Present results show the computational difficulties in studying the coordination properties of metal complexes from static calculations and highlight the importance of explicitly including a sufficient number of water molecules that allow representing the hydrogen bond network around the complex as well as the metal-water interactions.

Acknowledgements

The authors gratefully acknowledge financial support from MINECO, through CTQ2014-59544-P and CTQ2011-24847 projects, and the Generalitat de Catalunya (2014SGR-482 project), and the use of computer time at the BSC supercomputing center (QCM-2012-1-0021 and QCM-2012-2-0026 projects). MS also acknowledges support through 2011 ICREA Academia award.

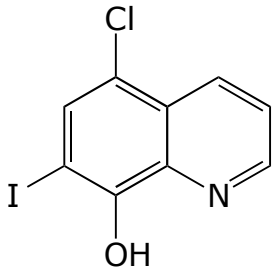

Scheme 1

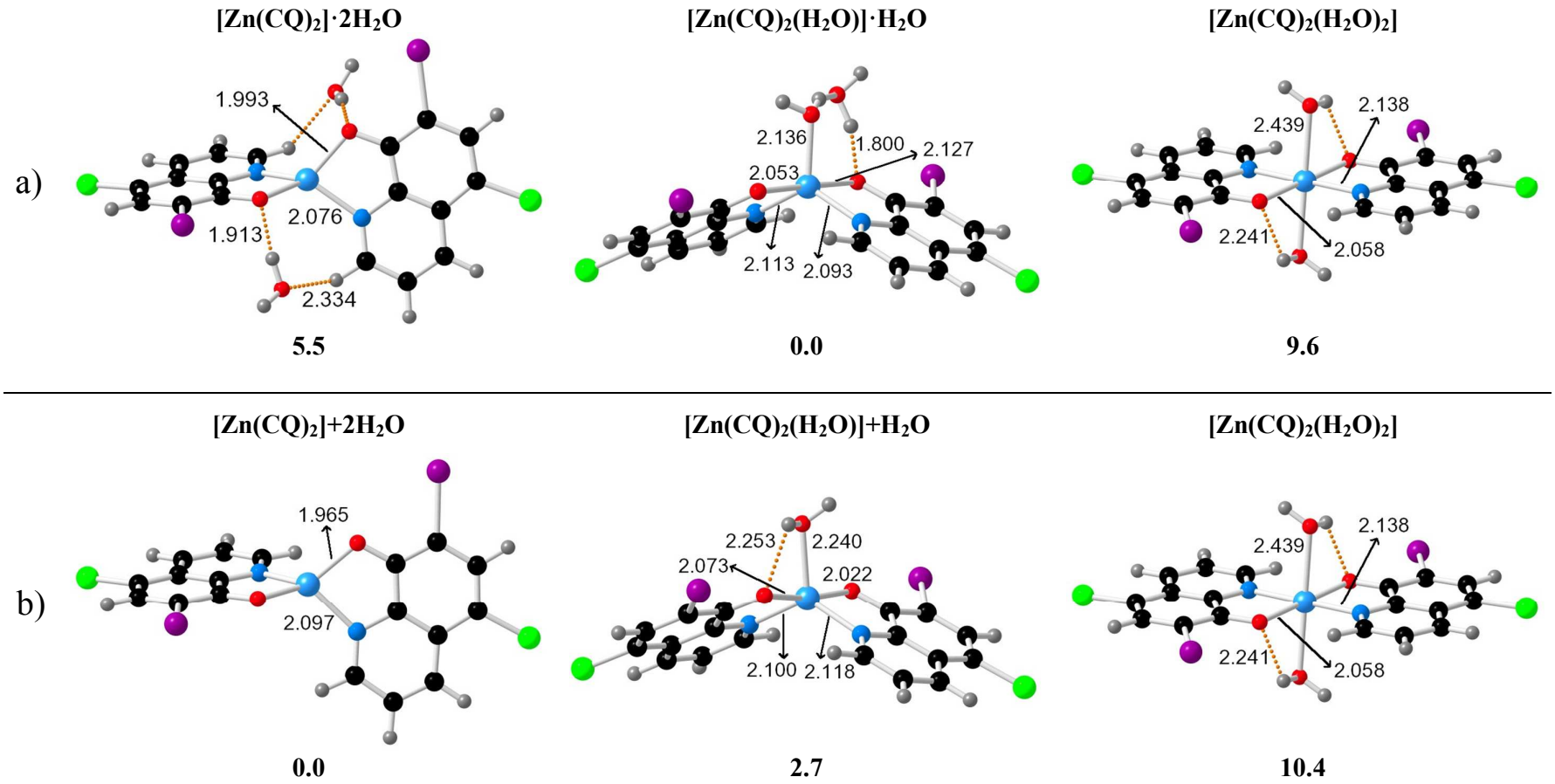

Figure 1. BLYP gas phase optimized geometries of the most stable isomers of $[Zn(CQ)_2(H_2O)_{2-n}]\cdot nH_2O$ (a) and $[Zn(CQ)_2(H_2O)_n]$ (b) complexes with n = 0, 1 and 2. Distances are in Å and relative free energies (ΔG^0_{gas}) in kcal mol^{-1}.

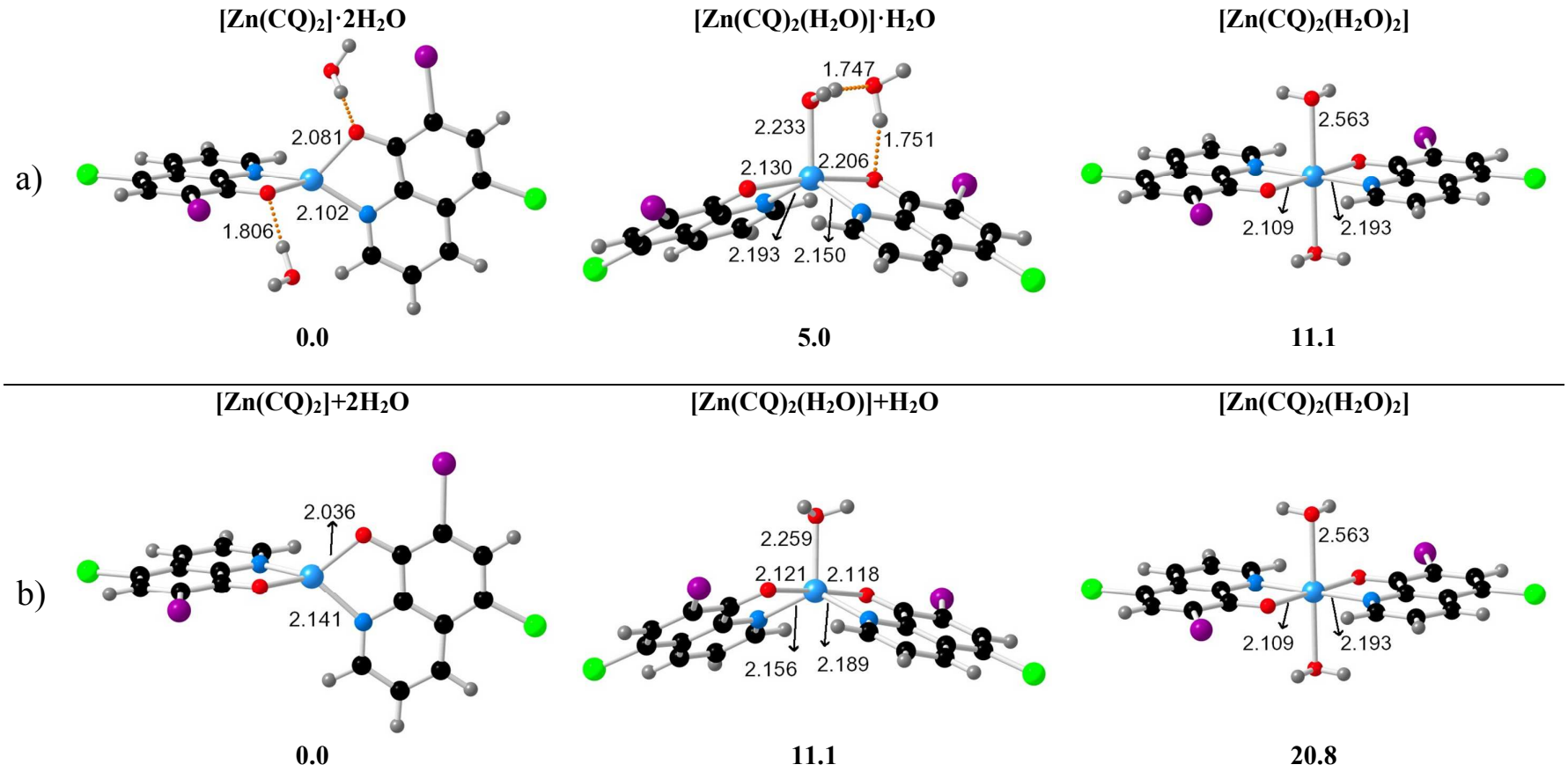

Figure 2. BLYP solution phase (SMD method) optimized geometries of the isomers of $[Zn(CQ)_2(H_2O)_{2-n}]\cdot nH_2O$ (a) and $[Zn(CQ)_2(H_2O)_n]$ complexes (b) with n = 0, 1 and 2. Distances are in Å and relative free energies (ΔG^*_{sol}) in kcal mol^{-1}. [a]In the case $[Zn(CQ)_2]\cdot 2H_2O$ an alternative structure 2.1 kcal mol^{-1} more stable has been found (see Supplementary Information), however we show the structure equivalent to that found in gas phase.

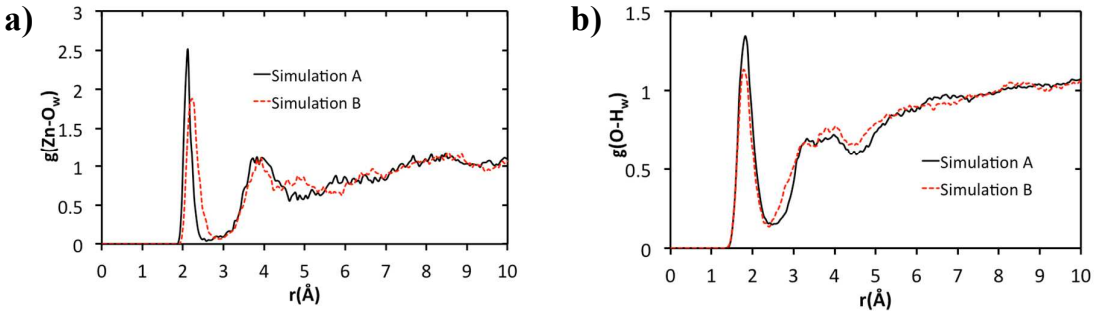

Figure 3. Radial distribution of water with respect to the Zn (a) and O (b) atoms of the complex for $[Zn(CQ)_2H_2O]$ (simulation A) and $[Zn(CQ)_2]$ (simulation B).

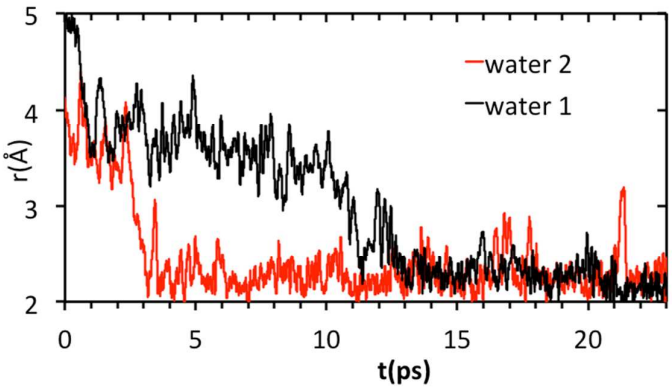

Figure 4. Fluctuations of the distance Zn···O$_w$ of two solvent molecules from simulation B ($[ZnCQ_2]$).

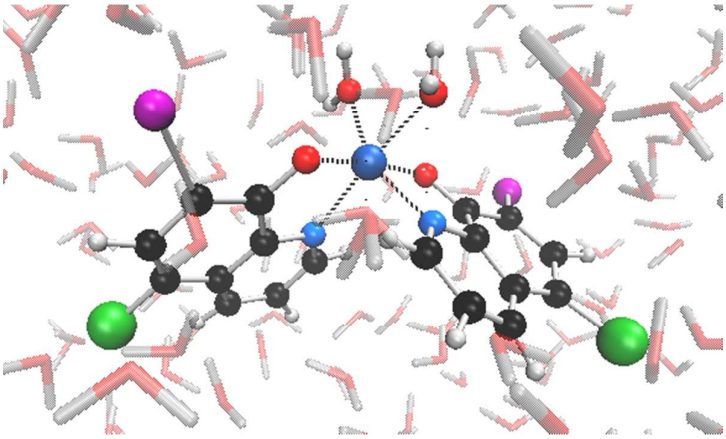

Figure 5. Snapshot of the complex at the end of simulation B ([$ZnCQ_2$]).

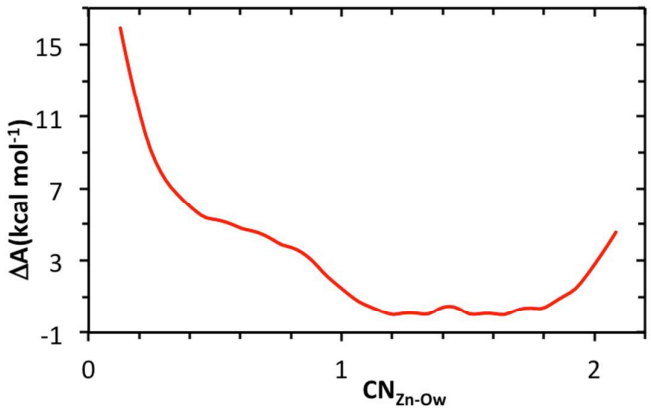

Figure 6. Free energy profile as a function of the Zn-Ow coordination number.

References

1 J. Hardy and D. J. Selkoe, *Science*, 2002, **297**, 353–356.

2 M. A. Lovell, J. D. Robertson, W. J. Teesdale, J. L. Campbell and W. R. Markesbery, *J. Neurol. Sci.*, 1998, **158**, 47–52.

3 D. P. Smith, G. D. Ciccotosto, D. J. Tew, M. T. Fodero-Tavoletti, T. Johanssen, C. L. Masters, K. J. Barnham and R. Cappai, *Biochemistry*, 2007, 2881–2891.

4 C. S. Atwood, R. D. Moir, X. Huang, R. C. Scarpa, N. M. E. Bacarra, D. M. Romano, M. A. Hartshorn, R. E. Tanzi and A. I. Bush, *J. Biol. Chem.*, 1998, **273**, 12817–12826.

5 R. A. Cherny, J. T. Legg, C. A. McLean, D. P. Fairlie, X. Huang, C. S. Atwood, K. Beyreuther, R. E. Tanzi, C. L. Masters and A. I. Bush, *J. Biol. Chem.*, 1999, **274**, 23223–23228.

6 L. E. Scott and C. Orvig, *Chem. Rev.*, 2009, **109**, 4885–910.

7 P. J. Crouch, A. R. White and A. I. Bush, *FEBS J.*, 2007, **274**, 3775–83.

8 K. Barnham, R. Cherny, R. Cappai, S. Melov, C. Masters and A. Bush, *Drug Des. Rev. - Online*, 2004, **1**, 75–82.

9 C. W. Ritchie, A. I. Bush, A. Mackinnon, S. Macfarlane, M. Mastwyk, L. MacGregor, L. Kiers, R. Cherny, Q.-X. Li, A. Tammer, D. Carrington, C. Mavros, I. Volitakis, M. Xilinas, D. Ames, S. Davis, K. Beyreuther, R. E. Tanzi and C. L. Masters, *Arch. Neurol.*, 2003, **60**, 1685–1691.

10 C. Rodríguez-Rodríguez, N. Sánchez de Groot, A. Rimola, A. Alvarez-Larena, V. Lloveras, J. Vidal-Gancedo, S. Ventura, J. Vendrell, M. Sodupe and P. González-Duarte, *J. Am. Chem. Soc.*, 2009, **131**, 1436–51.

11 M. Di Vaira, C. Bazzicalupi, P. Orioli, L. Messori, B. Bruni, P. Zatta, V. Uni and V. Lastruccia, *Inorg. Chem.*, 2004, **43**, 3795–3797.

12 L. Rulíšek and J. Vondrášek, *J. Inorg. Biochem.*, 1998, **71**, 115–127.

13 P. J. Stephens, F. J. Devlin, C. F. Chabalowski and M. J. Frisch, *J. Phys. Chem.*, 1994, **98**, 11623–11627.

14 A. D. Becke, *J. Chem. Phys.*, 1993, **98**, 5648–5652.

15 C. Lee, W. Yang and R. G. Parr, *Phys. Rev. B*, 1988, **37**, 785–789.

16 A. D. Becke, *Phys. Rev. A*, 1988, **38**, 3098–3100.

17 W. Koch and M. C. Holthausen, *A Chemist's Guide to Density Functional Theory*, Wiley-VCH, Weinheim, 2nd edn., 2001.

18 S. Miertuš, E. Scrocco and J. Tomasi, *Chem. Phys.*, 1981, **55**, 117–129.

19 V. Barone and M. Cossi, *J. Phys. Chem. A*, 1998, **102**, 1995–2001.

20 M. Cossi, N. Rega, G. Scalmani and V. Barone, *J. Comput. Chem.*, 2003, **24**, 669–81.

21 V. Barone, M. Cossi and J. Tomasi, *J. Chem. Phys.*, 1997, **107**, 3210–3221.

22 A. V Marenich, C. J. Cramer and D. G. Truhlar, *J. Phys. Chem. B*, 2009, **113**, 6378–96.

23 P. J. Hay and W. R. Wadt, *J. Chem. Phys.*, 1985, **82**, 299–310.

24 A. J. H. Wachters, *J. Chem. Phys.*, 1970, **52**, 1033–1036.

25 K. Raghavachari and G. W. Trucks, *J. Chem. Phys.*, 1989, **91**, 1062–1065.

26 P. J. Hay, *J. Chem. Phys.*, 1977, **66**, 4377–4384.

27 M. J. et al. Frisch, Gaussian, Inc., Wallingford CT, 2009.

28 J. VandeVondele, M. Krack, F. Mohamed, M. Parrinello, T. Chassaing and J. Hutter, *Comput. Phys. Commun.*, 2005, **167**, 103–128.

29 S. Grimme, J. Antony, S. Ehrlich and H. Krieg, *J. Chem. Phys.*, 2010, **132**, 154104.

30 D. Marx, M. Tuckerman, J. Hutter and M. Parrinello, *Nature*, 1999, 601–604.

31 a Pasquarello, I. Petri, P. S. Salmon, O. Parisel, R. Car, E. Toth, D. H. Powell, H. E. Fischer, L. Helm and a Merbach, *Science*, 2001, **291**, 856–9.

32 Y. Wu, H. L. Tepper and G. A. Voth, *J. Chem. Phys.*, 2006, **124**, 024503.

33 W. L. Jorgensen, D. S. Maxwell and J. Tirado-Rives, *J. Am. Chem. Soc.*, 1996, **118**, 11225–11236.

34 C. I. Bayly, P. Cieplak, W. Cornell and P. A. Kollman, *J. Phys. Chem.*, 1993, **97**, 10269–10280.

35 W. G. Hoover, 1985, **31**, 1695–1697.

36 S. Nosé, *Mol. Phys.*, 1984, **52**, 255–268.

37 J. VandeVondele, F. Mohamed, M. Krack, J. Hutter, M. Sprik and M. Parrinello, *J. Chem. Phys.*, 2005, **122**, 14515.

38 M. V Fernández-Serra and E. Artacho, *J. Chem. Phys.*, 2004, **121**, 11136–44.

39 G. Lippert, J. Hutter and M. Parrinello, *Mol. Phys.*, 1997, **92**, 477–488.

40 J. VandeVondele and J. Hutter, *J. Chem. Phys.*, 2007, **127**, 114105.

41 M. Krack, *Theor. Chem. Acc.*, 2005, **114**, 145–152.

42 S. Goedecker, M. Teter and J. Hutter, *Phys. Rev. B*, 1996, **54**, 1703–1710.

43 J. VandeVondele and J. Hutter, *J. Chem. Phys.*, 2003, **118**, 4365.

44 M. Iannuzzi, A. Laio and M. Parrinello, *Phys. Rev. Lett.*, 2003, **90**, 238302.

45 J. Kästner and W. Thiel, *J. Chem. Phys.*, 2005, **123**, 144104.

46 B. Ensing, M. De Vivo, Z. Liu, P. Moore and M. L. Klein, *Acc. Chem. Res.*, 2006, **39**, 73–81.

47 A. Laio and M. Parrinello, *Proc. Natl. Acad. Sci. U. S. A.*, 2002, **99**, 12562–6.

48 A. Melchior, M. Tolazzi, J. M. Martínez, R. R. Pappalardo and E. Sánchez Marcos, *J. Chem. Theory Comput.*, 2015, DOI: 10.1021/ct500975a.

49 V. S. Bryantsev, M. S. Diallo and W. a Goddard, *J. Phys. Chem. A*, 2009, **113**, 9559–67.

50 L. A. Truflandier and J. Autschbach, *J. Am. Chem. Soc.*, 2010, **132**, 3472–3483.